

Adsorption of Ne on alkali surfaces studied with a density functional theory

Salvador A. Sartarelli,¹ Leszek Szybisz,^{2,3,4,*} and Ignacio Urrutia^{2,3,4}

¹*Instituto de Desarrollo Humano, Universidad Nacional de General Sarmiento, Gutierrez 1150, RA-1663 San Miguel, Argentina*

²*Laboratorio TANDAR, Departamento de Física, Comisión Nacional de Energía Atómica, Av. del Libertador 8250, RA-1429 Buenos Aires, Argentina*

³*Departamento de Física, Facultad de Ciencias Exactas y Naturales, Universidad de Buenos Aires, Ciudad Universitaria, RA-1428 Buenos Aires, Argentina*

⁴*Consejo Nacional de Investigaciones Científicas y Técnicas, Av. Rivadavia 1917, RA-1033 Buenos Aires, Argentina*

(Received 8 October 2008; published 14 January 2009)

A density functional formalism is applied to investigate the wetting behavior of Ne adsorbed on planar substrates. The study is performed over the complete range of temperatures spanned from the triple point T_t up to the critical one T_c . For this purpose, an effective attractive pair potential was built on the basis of a separation procedure. This approach yields a good description of properties of the liquid-vapor interface at coexistence in the whole range of temperatures $T_t \leq T \leq T_c$. The adsorption of Ne on alkali metals and the alkaline-earth metal Mg is analyzed. This sequence of substrates exhibit increasing attractive strength leading to a variety of wetting situations throughout the interval $T_t \leftrightarrow T_c$. A comparison with experimental data and other microscopic calculations is done. The predictions of a simple model are discussed. For Ne/Rb we were able to resolve prewetting lines. Results obtained from a density functional are reported for Ne/K and Ne/Mg. In the case of the latter system the interesting behavior occurs close to T_t . According to our results, Ne wets surfaces of Na and Li, and this statement is in agreement with the whole picture of the analyzed substrates.

DOI: [10.1103/PhysRevE.79.011603](https://doi.org/10.1103/PhysRevE.79.011603)

PACS number(s): 68.08.Bc, 61.20.Ne, 64.70.F-

I. INTRODUCTION

Fluids in the presence of solid substrates develop liquid-vapor interfaces. Knowledge of the phase behavior is fundamental for testing theoretical microscopic models as well as for devising practical applications in fields from oil recovery to biology. Therefore, for many decades, this matter has been a topic of much interest. Let us now describe the current picture of the physisorption of a liquid phase (l) on a solid substrate (s) in the presence of a vapor atmosphere (v). Both involved fluid phases, i.e., the bulk liquid l and vapor v , coexist at temperature T when the chemical potential μ and the pressure P equal the corresponding saturation values $\mu_0(T)$ and $P_0(T)$. The latter quantities define l - v coexistence lines in the μ - T and P - T planes for temperatures spanning from the triple point T_t to the critical one T_c . Let us assume a planar geometry and denote as $U_{sf}(z)$ the solid-fluid interaction, where z is the distance perpendicular to the surface. When the strength of the substrate is moderate (i.e., if the wall-fluid attraction is not much bigger than the fluid-fluid one) there is a first-order wetting transition at the point $[T_w, \mu_w = \mu_0(T_w)]$ below T_c . T_w is characterized by the appearance of coexisting thin and very thick adsorbed fluid films. For $T < T_w$ the coverage of adsorbed films is finite (incomplete wetting). When measured in nominal layers ℓ , the coverage or excess surface density becomes

$$\Gamma_\ell = \frac{1}{[\rho_l(T)]^{2/3}} \int_0^\infty dz [\rho(z) - \rho_B], \quad (1.1)$$

where $\rho(z)$ is the density profile, $\rho_B = \rho(z = \infty)$ the asymptotic bulk density, which is usually the vapor density at saturation

$\rho_v(T)$, and $\rho_l(T)$ the liquid density at saturation. For temperatures higher than T_w there is an associated prewetting line which extends away from $[T_w, \mu_0(T)]$ into the region of pressures below the bulk saturation value at a given temperature, $P_0(T)$. The locus of this line in the plane T - μ is determined by $\mu_{pw}(T) = \mu_0(T) + \Delta\mu_{pw}(T)$. A schematic phase diagram is depicted in Fig. 3 of [1], where it is shown that the line of prewetting transitions terminates in a surface critical point (T_{cpw}, μ_{cpw}) . A prewetting transition is marked by a jump in Γ_ℓ (see, e.g., Fig. 9 in [2]). This discontinuity in Γ_ℓ vanishes at T_{cpw} , where the coexisting thin and thick films become identical. For $T > T_{cpw}$ the adsorbed stable film grows continuously for increasing coverage. If the tail of the adsorption potential has the van der Waals form, i.e., $U_{sf}(z) \approx -C/z^3$, then the following useful form for determining T_w may be derived from thermodynamic arguments [3]:

$$\Delta\mu_{pw}(T) = a_{pw}(T - T_w)^{3/2}. \quad (1.2)$$

Here a_{pw} is a model parameter. For strong substrates the wetting may be observed at T_t or at even lower temperatures.

Experimentally, these first-order surface phase transitions have been extensively measured for ^4He adsorbed on alkali-metal substrates (a survey of references is given in [4]). Prewetting transitions of H_2 films on Rb and Cs have been also observed [3,5,6]. Hess, Sabatini, and Chan (HSC) [7] measured the behavior of Ne in the presence of Rb and Cs at temperatures up to the fluid critical point $T_c = 44.4$ K. They found for Ne/Rb incomplete wetting for $T \leq 42.96$ K and wetting growth for $T \geq 43.44$ K. In the case of Ne/Cs no wetting was seen all the way to T_c . On the other hand, triple point wetting has been measured in the cases of Ar/Au [8] and Xe/NaF [9].

Microscopic theoretical studies of the adsorption of classical fluids are performed by applying density functional

*Corresponding author; szybisz@tandar.cnea.gov.ar

TABLE I. Wetting properties of Ne adsorbed on alkali-metal substrates. The ratio D/ε_{ff} , wetting, T_w , and prewetting critical T_{cpw} temperatures are listed. PW stands for present work, DR for drying, and NW for nonwetting.

Wall	D/ε_{ff}	I_u (K Å) CCZ ^a	Expt. ^b	SM ^a	T_w (K) GCMC ^{c,d}	DF ^e	DF (PW)	a_{pw}/k_B (K ^{-1/2}) DF (PW)	GCMC ^c	T_{cpw} (K) DF ^e	DF (PW) ^f
Cs	0.70	78.3	NW	38							
Rb	0.71	78.6	43.4	38	DR	44	42.2	-0.16			43.5
K	0.84	82.4		38			41.9	-0.16			43
Na	1.10	107		36	NW	40	39.1	-0.20		44	42
Li	1.49	135		33	NW	38	35.5	-0.24		41	39
Mg	2.79	212		26	22		20.5	-0.26	31		30

^aReference [19]

^bReference [7]

^cReference [14]

^dReference [15]

^eReference [17]

^fThese values are upper limits for the critical prewetting temperatures.

(DF) theories, Monte Carlo (MC) computer simulations, and molecular dynamics (MD). Good summaries of these approaches may be found, e.g., in [10–13]. We started a project to study quantitatively the wetting near T_t by using a DF theory. As a first step, we have undertaken the analysis of the prewetting behavior in the adsorption of Ne on Mg, for which grand canonical MC (GCMC) simulations [14,15] indicate that there is already wetting at $T_t=24.55$ K. However, when we carried out calculations by utilizing the formalism proposed by Kierlik and Rosinberg (KR) [16] in conjunction with the effective pair potential suggested by Ancilotto *et al.* [17,18], it was impossible to get convergence of the solutions close to the triple point due to the appearance of divergent oscillations in the numerical procedure. In order to overcome this shortcoming we sought for the source of the trouble, finding that it originates in the choice for the attractive part of the fluid-fluid interaction.

It is the aim of the present work to propose an effective pair potential and to report results of its application in a rather comprehensive study of the adsorption of Ne on alkali metals and the alkaline-earth metal Mg. According to a simple model (SM) [2] that compares the energy cost of forming a thick film (surface tension) with the benefit due to the vapor-surface attractive interaction, the wetting condition is

$$\begin{aligned}
 & -[\rho_l(T) - \rho_v(T)] \int_{z_{\min}}^{\infty} dz U_{sf}(z) \\
 & = -[\rho_l(T) - \rho_v(T)] I_u \geq 2\gamma_{lv}(T). \quad (1.3)
 \end{aligned}$$

Here z_{\min} is the location of the minimum of $U_{sf}(z)$ and $\gamma_{lv}(T)$ is the liquid-vapor surface tension at saturation. Chishaya, Cole, and Zaremba (CCZ) [19] estimated T_w by inserting in Eq. (1.3) their own adsorption potential. The results are included in Table I and indicate that Ne wets all the substrates mentioned above. In the literature there are reports of further investigations on these systems. There are experimental data and theoretical estimations indicating that Ne wets Rb below T_c as quoted in Table I, but there are not calculations showing a prewetting regime. In the case of Ne/K neither experimental work nor microscopic calcula-

tions have been published. For the Ne/Na and Ne/Li systems, there are contradictory statements: the DF calculations of Ancilotto and Toigo (AT) [17] suggest wetting below T_c in both cases, while Bojan *et al.* [14] arrived at the contrary conclusion on the basis of GCMC simulations as indicated in Table I. Finally, for the Ne/Mg system although GCMC simulations [14] indicate a prewetting line close to T_t (see Table I) no DF calculations have been published.

The paper is organized in the following way. The main features of the density functional for classical fluids are summarized in Sec. II, where we also present the alternative effective pair potential which yields values of the liquid-vapor surface tension in agreement with experimental data. In Sec. III we describe the results for the wetting behavior of Ne adsorbed on alkali-metal surfaces. In this analysis one covers the whole range of temperatures $T_t \leq T \leq T_c$. Finally, a summary is given in Sec. IV.

II. THEORETICAL FORMALISM

A. Density functional theory

Let us first outline the main features of a mean field DF theory. In such a formalism the Helmholtz free energy $F[\rho(\mathbf{r})]$ of an inhomogeneous fluid is written as a functional of the local density $\rho(\mathbf{r})$ (see, e.g., [10]):

$$\begin{aligned}
 F[\rho(\mathbf{r})] = & \nu_{id} k_B T \int d\mathbf{r} \rho(\mathbf{r}) \{ \ln[\Lambda^3 \rho(\mathbf{r})] - 1 \} \\
 & + \int d\mathbf{r} \rho(\mathbf{r}) f_{HS}[\bar{\rho}(\mathbf{r}); d_{HS}] \\
 & + \frac{1}{2} \int \int d\mathbf{r} d\mathbf{r}' \rho(\mathbf{r}) \rho(\mathbf{r}') \Phi_{attr}(|\mathbf{r} - \mathbf{r}'|) \\
 & + \int d\mathbf{r} \rho(\mathbf{r}) U_{sf}(\mathbf{r}). \quad (2.1)
 \end{aligned}$$

The first term is the ideal gas free energy, where k_B is the Boltzmann constant, $\Lambda = \sqrt{2\pi\hbar^2/mk_B T}$ is the thermal de Broglie wavelength of the molecule of mass m , and ν_{id} is a parameter introduced in Eq. (2) of [18] (in the standard

theory it is equal to unity). The second term takes into account the repulsive fluid-fluid interaction approximated by a hard-sphere (HS) functional with a certain choice of the HS diameter d_{HS} . The third term involves the attractive fluid-fluid interaction $\Phi_{\text{attr}}(|\mathbf{r}-\mathbf{r}'|)$ treated in a mean field approximation (MFA). The last contribution stands for the effect of the solid-fluid potential $U_{\text{sf}}(\mathbf{r})$. In the present work we shall use for $f_{\text{HS}}[\bar{\rho}(\mathbf{r}); d_{\text{HS}}]$ the expression provided by the nonlocal DF theory of KR [16], where $\bar{\rho}(\mathbf{r})$ is an averaged density.

B. Effective attractive pair potential

For MD and GCMC calculations it is commonly assumed that fluid particles interact via a spherically symmetric Lennard-Jones (LJ) 12-6 potential $V_{\text{LJ}}(r)=4\epsilon_{\text{ff}}[(\sigma_{\text{ff}}/r)^{12}-(\sigma_{\text{ff}}/r)^6]$ with standard energy and size parameters. Such calculations performed with the standard depth and size parameters yield a fairly good phase diagram. However, in the case of a mean-field theory like the DF of Eq. (2.1), where for the two-body distribution function one assumes

$$\rho^{(2)}(\mathbf{r}, \mathbf{r}') = g(\mathbf{r}, \mathbf{r}')\rho(\mathbf{r})\rho(\mathbf{r}') \approx \rho(\mathbf{r})\rho(\mathbf{r}') \quad (2.2)$$

neglecting the correlation structure given by $g(\mathbf{r}, \mathbf{r}')$, the use of a bare LJ interaction leads to a far too low critical temperature T_c compared with the experimental value. The coexistence curve may be determined by using expressions for P and μ provided by Eq. (2.1) in the case of a uniform fluid of density ρ ,

$$P(T) = P_{\text{HS}}(T) + \frac{b}{2}\rho^2 \quad \text{and} \quad \mu(T) = \mu_{\text{HS}}(T) + b\rho, \quad (2.3)$$

with $b = \int d\mathbf{r} \Phi_{\text{attr}}(r)$. In the present work, P_{HS} and μ_{HS} were evaluated by using the compressibility expressions of Percus-Yevick [20] which are compatible with the KR formulation. When $\Phi_{\text{attr}}(r)$ is the attractive part of the bare LJ potential one gets $b_{\text{LJ}} = -(32\pi/9)\epsilon_{\text{ff}}\sigma_{\text{ff}}^3$. At coexistence the pressure as well as the chemical potential of the vapor and liquid phases should be equal

$$P(\rho_v) = P(\rho_l) \quad \text{and} \quad \mu(\rho_v) = \mu(\rho_l). \quad (2.4)$$

By imposing these conditions on Ne, the bare LJ with the standard parameters $\epsilon_{\text{ff}}/k_B = 33.9$ K and $\sigma_{\text{ff}} = 2.78$ Å leads to a coexistence curve significantly lower than the experimental one taken from Table III of [21]. In order to study quantitatively the adsorption of fluids within a DF approach one must require that the experimental bulk equation of state and liquid-vapor surface tension γ_{lv} be reproduced as well as possible in the whole range of temperatures $T_i \leq T \leq T_c$.

In the frame of the MFA Ancilotto and Toigo (AT) [17] have built up a $\Phi_{\text{attr}}(r)$ by starting from the proposal of Bruno, Caccamo, and Tarazona (BCT) given in Eq. (17) of [22] and considering the size parameter of the potential as an effective temperature depending quantity, $\tilde{\sigma}_{\text{ff}}$,

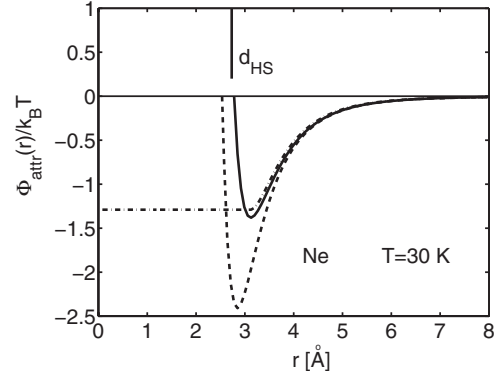


FIG. 1. Attractive part of the LJ potential for Ne as a function of the interatomic distance. The solid curve is the bare LJ potential. The dashed and dash-dotted lines are the BCT-AT and WCA-PW approaches, respectively. The vertical line indicates the position of d_{HS} .

$$\Phi_{\text{attr}}^\lambda(r) = \begin{cases} 0, & r \leq \lambda^{1/6} \tilde{\sigma}_{\text{ff}} \\ 4\epsilon_{\text{ff}} \left[\lambda \left(\frac{\tilde{\sigma}_{\text{ff}}}{r} \right)^{12} - \left(\frac{\tilde{\sigma}_{\text{ff}}}{r} \right)^6 \right], & r > \lambda^{1/6} \tilde{\sigma}_{\text{ff}}. \end{cases} \quad (2.5)$$

The BCT form has been devised to describe the effect of the peak in the pair correlation function $g(r=|\mathbf{r}-\mathbf{r}'|)$ occurring about the minimum of $V_{\text{LJ}}(r)$. In Eq. (2.5) there are two free parameters λ and $\tilde{\sigma}_{\text{ff}}$, while in the original version of Ref. [22] it was kept $\tilde{\sigma}_{\text{ff}} = \sigma_{\text{ff}}$. For $\lambda=1$ one recovers the standard LJ form, while for $\lambda < 1$ the value at the minimum is increased by a factor λ^{-1} . In this BCT-AT approach one gets $b_\lambda = (32\pi/9\sqrt{\lambda})\epsilon_{\text{ff}}\tilde{\sigma}_{\text{ff}}^3$. In order to determine the three adjustable parameters (i.e., ν_{id} , λ , and $\tilde{\sigma}_{\text{ff}}$), Ancilotto *et al.* [18] set $d_{\text{HS}} = \tilde{\sigma}_{\text{ff}}$ and imposed at each temperature T the conditions of Eq. (2.4) together with the requirement that the quantities ρ_v , ρ_l , and $P(\rho_v) = P(\rho_l) = P_0$ be equal to the values quoted in Table III of Ref. [21]. Figure 1 shows the BCT-AT attractive part of the interaction compared with the bare LJ potential at $T=30$ K.

The surface tension of the liquid-vapor interface is calculated from symmetric free slabs according to

$$\gamma_{lv} = \frac{1}{2}[(\Omega + P_0 V)/A] = \frac{1}{2}[\Omega/A + P_0 L], \quad (2.6)$$

where $\Omega = F - \mu N$ is the grand potential of the system, A the area of the interface, and L the size of the box adopted for solving DF equations. Figure 2 shows the experimental data for Ne [18,23] together with the prediction from the fluctuation theory of critical phenomena [13],

$$\gamma_{lv} = \gamma_{lv}^0 (1 - T/T_c)^{1.26}, \quad (2.7)$$

with $\gamma_{lv}^0 = 11.35$ K/Å². In addition, the results computed by using the KR-BCT-AT approach [18] are also plotted. As mentioned before we could not obtain convergence of solutions close to T_i when using such an approach; moreover, no results are reported in that Letter [18] for temperatures lower than $T=30$ K where there are experimental data. We found that the appearance of diverging oscillations of the density

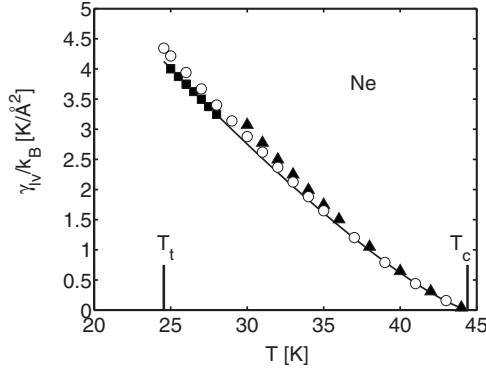


FIG. 2. Surface tension of Ne as a function of temperature. Full squares are the experimental data as displayed in Fig. 1(b) of Ref. [18], triangles and circles were calculated by using the BCT-AT and WCA-PW separations. The solid curve corresponds to the fluctuation theory of critical phenomena (see text).

profile in the KR-BCT-AT approach prevents the convergence of the solutions close to T_t . The wavelength of these oscillations is $\lambda_p = 0.95\tilde{\sigma}_{ff}$. Hence, it would be plausible to assume a relation to the sharp peak exhibited by the BCT-AT pair potential in Fig. 1. The relative importance of this peak in the total free energy given by $\Phi_{\text{attr}}^\lambda(r)/k_B T$ increases for decreasing temperatures; in turn, due to this effect the fluid could undergo a too early “freezing” above the experimental T_t . In other words, a too strong enhancement of the attraction produces an upward shift of the triple point temperature. This could be the source for the failure in convergence because a solid phase should be treated in a different way [16].

It is important to mention that this effect has already been discussed by Mederos *et al.* [24]. These authors emphasize the different role played by the one-body, $\rho(\mathbf{r})$, and two-body, $\rho^{(2)}(\mathbf{r}, \mathbf{r}')$, distribution functions in systems with uniform density and in systems with structured densities. They suggest improving the representation of the pair distribution function by introducing an exact “local-compressibility” relation together with an approximated “local-thermodynamics” expression for the isothermal compressibility given by their Eqs. (3) and (4), respectively. This perturbation treatment solves the troubles from the root yielding a phase diagram in agreement with Monte Carlo simulation studies (see Fig. 2 in [24]). However, its implementation for inhomogeneous systems would require large, time-consuming calculations.

In order to avoid the shortcoming of the KR-BCT-AT approach without increasing the computational effort, we stay with the MFA and propose to use the following form for the effective attractive part of the fluid-fluid interaction:

$$\Phi_{\text{attr}}^{\text{WCA}}(r) = \begin{cases} -\tilde{\epsilon}_{ff}, & r \leq 2^{1/6}\tilde{\sigma}_{ff}, \\ 4\tilde{\epsilon}_{ff} \left[\left(\frac{\tilde{\sigma}_{ff}}{r} \right)^{12} - \left(\frac{\tilde{\sigma}_{ff}}{r} \right)^6 \right], & r > 2^{1/6}\tilde{\sigma}_{ff}, \end{cases} \quad (2.8)$$

It is based on the separation introduced by Weeks, Chandler, and Andersen (WCA) in their perturbation theory of fluids [25] (see Fig. 1 therein). Here the effect of $g(r)$ is spread

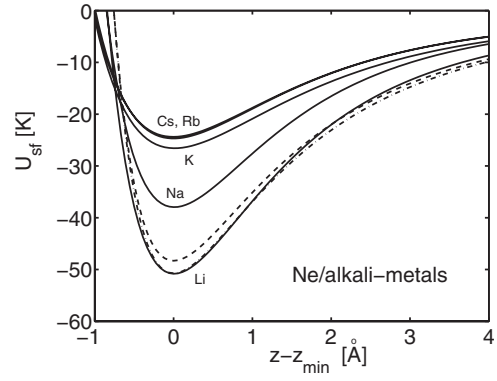


FIG. 3. Comparison of adsorption potentials of Ne on alkali-metal substrates; the curves are centered at the corresponding minimum. The labeled solid curves are CCZ potentials. The dashed and dashed-dotted curves are the S10-4 potentials for Ne/Li corresponding to well depths $D=48$ and 50 K, respectively.

over a range of r similar to that used for evaluating $\bar{\rho}(\mathbf{r})$. This effective interaction also preserves the long-range behavior $-r^{-6}$ of the original bare potential, which is important when studying adsorption properties. In the present WCA (WCA-PW) method, we consider $\tilde{\epsilon}_{ff}$ and $\tilde{\sigma}_{ff}$ as free parameters. In this case one gets $b_{\text{PW}} = -(32\sqrt{2}\pi/9)\tilde{\epsilon}_{ff}\tilde{\sigma}_{ff}^3$. Since P and μ given in Eq. (2.3) depend on the integral of $\Phi_{\text{attr}}(r)$, the factor $\sqrt{2}\tilde{\epsilon}_{ff}$ plays the same role as $\epsilon_{ff}/\sqrt{\lambda}$. However, as shown in Fig. 1, the potentials as a function of r are very different. As we shall see later, this difference has an important effect when calculating the surface tension. It is important to notice that the WCA form when computed with the bare values ϵ_{ff} and σ_{ff} overestimates T_c as shown in Fig. 2 of [10]. The free parameters of the present DF (ν_{id} , $\tilde{\epsilon}_{ff}$, and $\tilde{\sigma}_{ff}$) were determined in the same way as was done by Ancilotto *et al.* [18]. The obtained $\Phi_{\text{attr}}^{\text{WCA}}(r)$ at $T=30$ K is also displayed in Fig. 1, where one may realize the difference between the two effective potentials. The KR-WCA-PW results for γ_{lv} are plotted in Fig. 2, where one may observe that our prediction is in very good agreement with experimental data and renormalization results throughout the whole range of temperatures $T_t \leq T \leq T_c$.

III. ANALYSIS OF WETTING PROPERTIES

The physisorption was analyzed by utilizing the *ab initio* potentials of Chismeshya, Cole, and Zaremba taking the parameters listed in Table 1 of [19]. Figure 3 shows the potentials exerted by the alkali-metal substrates. We shall discuss the DF results starting from the less attractive surfaces.

A. Alkali-metal substrates

Since the adsorption potential for Ne/Cs and Ne/Rb systems is ultraweak ($D/\epsilon_{ff} < 1$; see Table I) the interesting features of adsorption isotherms appear very near T_c . The results for Ne/Rb are displayed in Fig. 4, indicating that the wetting transition occurs slightly below $T=42.5$ K. By putting the obtained two values of $\Delta\mu$ in Eq. (1.2) we got $T_w=42.2$ K and $a_{\text{PW}}/k_B = -0.16$ K $^{-1/2}$. The critical prewetting point is

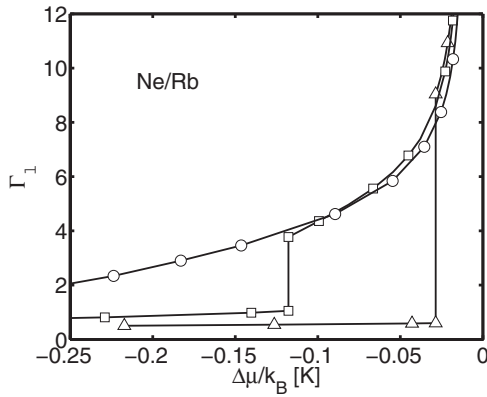


FIG. 4. Adsorption isotherms for the Ne/Rb system. $\Delta\mu$ is measured from the saturation value at liquid-vapor coexistence for Ne. $T=42.5$ K (triangles), 43 K (squares), and 43.5 K (circles).

about $T_{cpw} \approx 43.25$ K. All these values are quoted in Table I and the temperatures are in fair agreement with experimental data shown in Fig. 3 of HSC [7]. Ancilotto *et al.* [17,18] determined that the wetting transition occurs at $T \approx 43$ K, but stated that they were not able to resolve any prewetting line from their DF calculations. Here we present adsorption isotherms yielding a prewetting line for Ne/Rb as shown in Fig. 5. On the other hand, the obtained difference $T_{cpw} - T_w \approx 1$ K is in excellent agreement with experimental data [7].

In practice, our analysis of the Ne/Cs system yielded the same results as that for Ne/Rb, indicating wetting below T_c . This is due to the fact that the CCZ potentials for both systems are almost equal, as shown in Fig. 3. This result is in agreement with those of Ancilotto *et al.* [18], who suggested that in order to reproduce the experimental evidence for non-wetting found by HSC [7] the strength of the CCZ adsorption potential should be diminished. In view of these facts we do not include results for the Ne/Cs system in Table I.

The adsorption isotherms for the Ne/K system are displayed in Fig. 6. In this case the adsorption potential is slightly stronger than for the Ne/Rb system. Therefore, the isotherms for the same temperatures are shifted a bit toward more negative values of $\Delta\mu$, causing T_w to be below 42 K. One may observe a curious feature, namely, extreme jumps

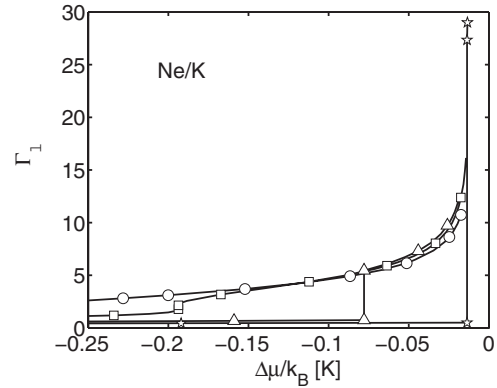


FIG. 6. Adsorption isotherms for the Ne/K system. $T=42$ K (stars), 42.5 K (triangles), 43 K (squares), and 43.5 K (circles).

in coverage occur just at the considered round temperatures, a small one of $\Delta\Gamma_\ell \approx 0.5$ at $T=43$ K and a rather large one of $\Delta\Gamma_\ell \approx 25$ at $T=42$ K. This behavior facilitates the determination of T_w and T_{cpw} . A fit to Eq. (1.2) yielded the values $T_w=41.9$ K and $a_{pw}/k_B=-0.16$ K^{-1/2}, which are also included in Table I together with T_{cpw} . The prewetting line is also displayed in Fig. 5, allowing a direct comparison with other substrates.

In the case of the Ne/Na and Ne/Li systems, we obtained similar adsorption isotherms to those displayed in Figs. 7 and 8 of AT [17]. The present prewetting lines are plotted in Fig. 5 and the results for T_w and T_{cpw} are included in Table I. These values are closer to T_c than to T_t . The small difference from those reported in Table III of AT [17] may be attributed to the use of different effective pair potentials, as well as different values of ν_{id} (notice that the possibility for $\nu_{id} \neq 1$ was introduced in a revised version of the DF formalism [18] published after AT). In any case, both DF studies indicate first-order wetting transitions followed by prewetting regimes, in disagreement with the GCMC results of [14,15]. In fact, the GCMC calculations of Bojan *et al.* [14] were performed by using an adsorption potential different from the CCZ. These authors utilized an interaction built by summing up contributions of planar sheets which originates a 10-4 potential (henceforth denoted as S10-4); the expression is given in Eq. (3) of their paper. In order to estimate the effect due to the use of different potentials, we calculated adsorption isotherms for Ne/Na and Ne/Li by using the S10-4 interaction within the framework of the present DF formalism. Since the results lead to the same conclusion for both systems, we shall report some results only for Ne/Li.

The S10-4 potential for the Ne/Li system evaluated for two values of the well depth D is plotted in Fig. 3. One is the value $D=48$ K adopted in [14], while the other $D=50$ K is the well depth of the CCZ potential. In the latter case, the S10-4 and CCZ potentials are very similar. The calculated chemical potentials for $T=38$ K are displayed in Fig. 7 as a function of coverage Γ_ℓ . Although there are shifts between the results corresponding to the three different potentials, in all the cases the isotherms indicate the existence of a prewetting regime signed by a jump in Γ_ℓ . After this jump for increasing coverage $\Delta\mu$ approaches monotonically zero from below. All these facts are evidence for a wetting transition.

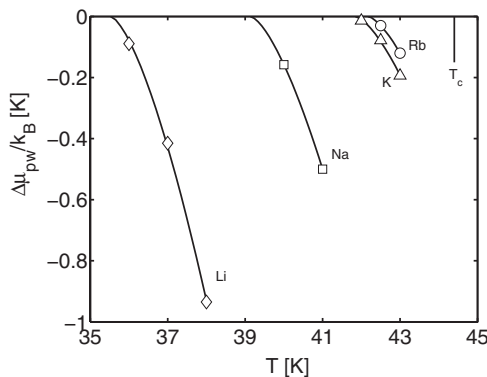


FIG. 5. Prewetting lines for Ne adsorbed on indicated alkali-metal substrates. The symbols are points calculated with DF while solid lines are given by Eq. (1.2) with the parameters quoted in Table I.

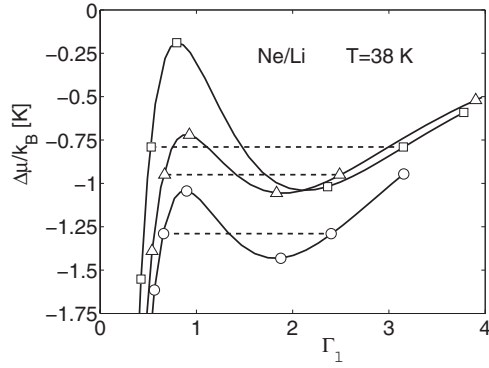


FIG. 7. Chemical potential measured from the saturation value for the Ne/Li system at $T=38$ K. The solid curve with triangles was obtained with the CCZ potential, while the curves with squares and circles were obtained with the S10-4 potential by setting $D=48$ and 50 K, respectively. In each case a dashed line indicates the Maxwell construction.

On the basis of the results described above we can state that DF calculations for Ne/Na and Ne/Li indicate first-order wetting transitions in both cases. This result is to be expected because Ne already wets the less attractive substrate of Rb below T_c . Hence, we would agree with the authors of the GCMC calculations [14] that such simulations were not able to discern prewetting regimes close to the critical point.

B. Substrate of the alkaline-earth metal Mg

The well depth of the adsorption potential for Ne on the alkaline-earth metal Mg is about $D=95$ K, double the attraction strength of a surface of Li. Hence, in this case one expects more adsorption and consequently a prewetting regime closer to T_t than to T_c . The corresponding S10-4 and CCZ potentials are very similar, as for Ne/Li with equal well depths.

Figure 8 shows density profiles of thin and thick films calculated at $T=28$ K compared with that obtained from

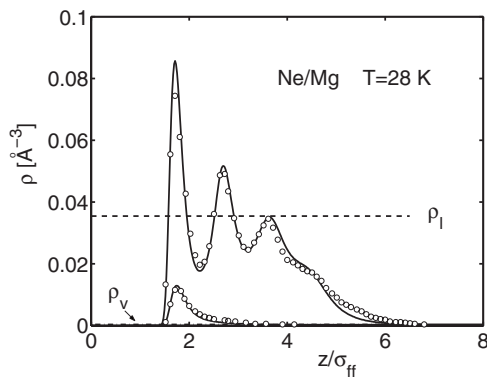


FIG. 8. Density profiles of films corresponding to two coverages in the case Ne/Mg at $T=28$ K. Thin films with $\Gamma_\ell=0.15$ and thick ones with $\Gamma_\ell=2.74$ are displayed. Solid curves are present results and open circles are GCMC data [14]. The dashed and dashed-dotted lines stand for the liquid $\rho_l=0.0355 \text{ \AA}^{-3}$ and vapor $\rho_v=0.0004 \text{ \AA}^{-3}$ densities for coexistence at this temperature.

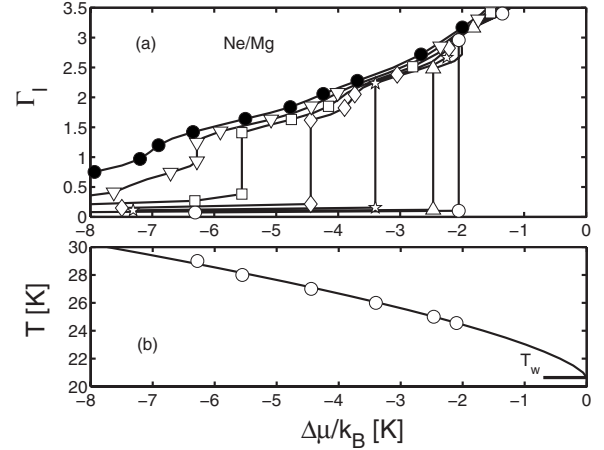


FIG. 9. (a) Adsorption isotherms for the Ne/Mg system; from right to left, the results correspond to temperatures $T=24.55, 25, 26, 27, 28, 29,$ and 30 K. (b) Dependence of $\Delta\mu_{pw}$ on temperature.

GCMC calculations [14]. The agreement between the two sets of profiles is quite good in spite of the fact that the adsorption potentials used are not the same; however, the energetics is slightly different. The ratio between the density of the DF first peak and the highest GCMC value is 1.15. In our case the plotted profiles lie in the stable regime; however, they do not correspond to coverages just before and after the prewetting jump due to some difference in the energetics of the CCZ and S10-4 potentials. The ratio of densities at the first peak and the first valley in Fig. 8 is 4.84; it increases for decreasing temperatures, reaching 5.46 at 26 K and 6.02 at the triple point 24.55 K. Let us provide some comments on the validity of the DF in this regime. On the basis of the study performed by Ravikovitch *et al.* [10] on the behavior of N_2 confined in slit carbon pores, we can state that our results are reliable. These authors utilized the raw WCA approach. The wall attraction for the N_2/C system is larger than in the Ne/Mg case, leading to a much more pronounced layering than that exhibited in our Fig. 8. Figure 8 of their paper shows a comparison of density profiles obtained with GCMC and DF calculations; in spite of the noticeable layering, the overall agreement is good, giving support to DF calculations. In passing, we may mention that the ratio between the first peaks obtained with DF and GCMC calculations shown in that plot is about 1.25, being slightly larger than our result.

The adsorption isotherms calculated for the Ne/Mg system are displayed in Fig. 9(a). We found that in this case the wetting transition occurs below T_t and the critical prewetting at $T_{cpw} \approx 29.5$ K. Figure 9(b) shows the dependence of $\Delta\mu_{pw}(T)$ on temperature. A nonlinear fit of the data to Eq. (1.2) yielded $T_w=20.5$ K and $a_{pw}=-0.26/k_B \text{ K}^{-1/2}$. This wetting temperature below T_t is in good agreement with the value $T_w=22$ K quoted in Table I of [15]. Furthermore, the difference $T_{cpw}-T_w$ coincides with that obtained from GCMC simulations [14]. On the other hand, for Ne/Mg the prewetting line measured in units of $\Delta\mu_{pw}$ is much larger than those corresponding to alkali metals.

C. Simple model

Let us now comment on some features of the SM. The values of I_u calculated by integrating CCZ potentials are

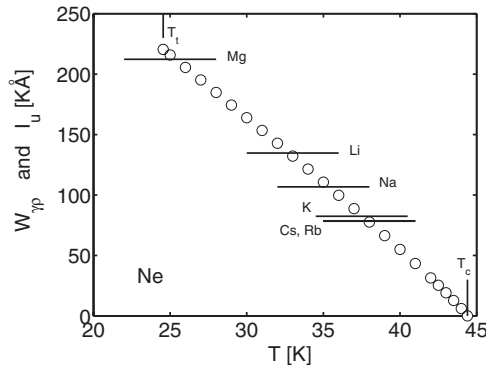


FIG. 10. Open circles are the ratios W_{γ_p} as a function of temperature needed to analyze wetting with the SM. Horizontal lines stand for I_u , T_i and T_c are also indicated.

quoted in Table I and displayed in Fig. 10. In order to have a better insight, instead of examining wetting by simply putting sets of $\gamma_{lv}(T)$, $\rho_l(T)$, and $\rho_v(T)$ into Eq. (1.3) as in a black box, it is convenient to rewrite that equation in a more elaborated way. According to Eq. (4) of [26] the wetting condition may be written as a condition for the integral I_u . Next, Eq. (2.7) for the liquid-vapor surface tension together with the simple and accurate Guggenheim's form $\rho_l(T) - \rho_v(T) = (7/2)\rho_c(1 - T/T_c)^{1/3}$ [see Eq. (6.4) in [23]; here, ρ_c is the fluid density at T_c] may be used to reduce the expression for the wetting condition. This procedure leads to

$$\begin{aligned} I_u &= - \int_{z_{\min}}^{\infty} dz U_{st}(z) \geq \frac{2\gamma_{lv}(T)}{\rho_l(T) - \rho_v(T)} \\ &= W_{\gamma_p}(T) = \frac{4\gamma_{lv}^0}{7\rho_c} (1 - T/T_c)^{0.93}. \end{aligned} \quad (3.1)$$

Figure 10 shows the ratio W_{γ_p} as a function of temperature. By looking at this figure one may verify that the condition of Eq. (3.1) leads to the values of T_w obtained by Chismesha *et al.* [19]. A glance at Table I indicates that the SM predicts fairly well the wetting for substrates of Na and Li, but in the cases of Rb, K, and Mg fails by several degrees. The failures for the ultraweak and for the stronger substrate are in opposite directions.

It is usually assumed that the wetting condition provided by the SM is applicable to any simple fluid adsorbed on an attractive surface. However, the structure of W_{γ_p} causes an important shortcoming. Since it reaches zero at T_c one could conclude that any surface exerting an attractive potential ($I_u > 0$) would be wetted by a fluid below T_c independently of how weak is the attraction. Hence, this SM is not capable of predicting a nonwetting phenomenon such as that observed for Ne/Cs [7]. Moreover, due to this feature the predicted T_w for Ne/Rb is significantly lower than the experimental value.

In order to get Eq. (1.3) Cheng *et al.* [2] approximated the free energy cost of creating a substrate-liquid interface, $\tilde{\gamma}_{sl}(T)$, by $\gamma_{lv}(T)$ introducing $\gamma_{lv}(T) + \tilde{\gamma}_{sl}(T) = 2\gamma_{lv}(T)$ in their Eq. (3.2). However, one can argue that such an assumption is

not valid close to T_c because at this critical temperature the substrate-liquid interface is still present and, therefore, $\tilde{\gamma}_{sl}(T)$ should not vanish for $T \rightarrow T_c$. In addition, it is plausible to expect that $\tilde{\gamma}_{sl}(T)$ should depend on the substrate, leading to sizable effects for all values of T . Furthermore, in the case of Ne/Mg close to T_i , when the integral $\int dz \rho(z) U_{st}(z)$ is approximated by $\rho_l \int dz U_{st}(z)$ one loses an important part of the contribution from the peak of the density profile (see Fig. 8) which occurs just at the minimum of the adsorption potential. The inclusion of this effect would lower T_w .

Although the predictions of the SM could be improved by taking into account the features described above, such a task goes beyond the scope of the present work.

IV. SUMMARY

An effective attractive part of the fluid-fluid interaction contributing to DF theories is proposed. It yields good quantitative results for the liquid-vapor surface tension at saturation for temperatures spanning from T_i to T_c , this was not possible when using a former proposal.

When the adsorption of Ne was analyzed, the known temperatures T_w and T_{cpw} in the whole range $T_i \leftrightarrow T_c$ are well reproduced. DF calculations for the Ne/K and Ne/Mg systems are reported. Prewetting lines for the adsorption on Rb, K, and Mg obtained from a DF formalism are presented. From Figs. 5 and 9(a) one concludes that the length of prewetting lines becomes larger for more attractive substrates. Predictions of a SM are discussed and some shortcomings are pointed out.

On the basis of all the described results we find it reasonable to state that Ne wets substrates of Na and Li, supporting the finding of Ancilotto and Toigo [17] against the evidence for nonwetting reported by Bojan *et al.* [14]. This controversy could be resolved experimentally. The predicted jumps in coverage occur at $|\Delta\mu_{pw}| \approx 0.5$ K for Na and at $|\Delta\mu_{pw}| \approx 1$ K for Li, yielding $P/P_0 = \exp(\Delta\mu_{pw}/k_B T) \approx 0.988$ and $P/P_0 \approx 0.975$, respectively. These values of the pressures could be in a range accessible for experiments similar to that performed very recently by van Cleve, Taborek, and Rutledge [27] for ^4He on Li.

Although we present results only for adsorption of Ne, the suggested $\Phi_{\text{attr}}^{\text{WCA}}(r)$ may also be used for other inert gases (Ar, Kr, and Xe), where similar problems with the BCT-AT expression appear near T_i . For instance, it could be utilized for studying adsorption of Xe on strong substrates like graphite covered by layers of Cs, which was already investigated by Curtarolo, Cole, and Diehl [28] with the GCMC technique. A possible immediate application of the present formulation is the analysis of the controversy between experimental data [9] and theoretical predictions [26] about the triple-point wetting of Xe on NaF.

ACKNOWLEDGMENTS

This work was supported in part by the Ministry of Culture and Education of Argentina through Grants CONICET PIP No. 5138/05, ANPCyT PICT No. 492 and No. 31980, and UBACYT No. X298.

- [1] R. Pandit, M. Schick, and M. Wortis, *Phys. Rev. B* **26**, 5112 (1982).
- [2] E. Cheng, M. W. Cole, J. Dupont-Roc, W. F. Saam, and J. Treiner, *Rev. Mod. Phys.* **65**, 557 (1993).
- [3] E. Cheng, G. Mistura, H. C. Lee, M. H. W. Chan, M. W. Cole, C. Carraro, W. F. Saam, and F. Toigo, *Phys. Rev. Lett.* **70**, 1854 (1993).
- [4] L. Szybisz, *Phys. Rev. B* **67**, 132505 (2003).
- [5] G. Mistura, H. C. Lee, and M. H. W. Chan, *J. Low Temp. Phys.* **96**, 221 (1994).
- [6] D. Ross, P. Taborek, and J. E. Rutledge, *Phys. Rev. B* **58**, R4274 (1998).
- [7] G. B. Hess, M. J. Sabatini, and M. H. W. Chan, *Phys. Rev. Lett.* **78**, 1739 (1997).
- [8] K. G. Sukhatme, J. E. Rutledge, and P. Taborek, *Phys. Rev. Lett.* **80**, 129 (1998).
- [9] L. Bruschi and G. Mistura, *Phys. Rev. B* **58**, 1181 (1998).
- [10] P. I. Ravikovitch, A. Vishnyakov, and A. V. Neimark, *Phys. Rev. E* **64**, 011602 (2001).
- [11] M. J. P. Nijmeijer, C. Bruin, A. F. Bakker, and J. M. J. van Leeuwen, *Phys. Rev. B* **44**, 834 (1991).
- [12] J. R. Henderson, P. Tarazona, F. van Swol, and E. Velasco, *J. Chem. Phys.* **96**, 4633 (1992).
- [13] J. Vrabec, G. K. Kedia, G. Fuchs, and H. Hasse, *Mol. Phys.* **104**, 1509 (2006).
- [14] M. J. Bojan, G. Stan, S. Curtarolo, W. A. Steele, and M. W. Cole, *Phys. Rev. E* **59**, 864 (1999); M. J. Bojan, W. W. Cole, I. K. Johnson, W. A. Steele, and Q. Wang, *J. Low Temp. Phys.* **110**, 653 (1998).
- [15] S. Curtarolo, G. Stan, M. J. Bojan, M. W. Cole, and W. A. Steele, *Phys. Rev. E* **61**, 1670 (2000).
- [16] E. Kierlik and M. L. Rosinberg, *Phys. Rev. A* **42**, 3382 (1990).
- [17] F. Ancilotto and F. Toigo, *Phys. Rev. B* **60**, 9019 (1999).
- [18] F. Ancilotto, S. Curtarolo, F. Toigo, and M. W. Cole, *Phys. Rev. Lett.* **87**, 206103 (2001).
- [19] A. Chizmeshya, M. W. Cole, and E. Zaremba, *J. Low Temp. Phys.* **110**, 677 (1998).
- [20] J. K. Percus and G. J. Yevick, *Phys. Rev.* **110**, 1 (1958).
- [21] V. A. Rabinovich, A. A. Vasserman, V. I. Nedostup, and L. S. Veksler, *Thermophysical Properties of Neon, Argon, Krypton, and Xenon* (Hemisphere, Washington, DC, 1988).
- [22] E. Bruno, C. Caccamo, and P. Tarazona, *Phys. Rev. A* **35**, 1210 (1987).
- [23] E. A. Guggenheim, *J. Chem. Phys.* **13**, 253 (1945).
- [24] L. Mederos, G. Navascués, P. Tarazona, and E. Chacón, *Phys. Rev. E* **47**, 4284 (1993).
- [25] J. D. Weeks, D. Chandler, and H. C. Andersen, *J. Chem. Phys.* **54**, 5237 (1971).
- [26] V. B. Shenoy and W. F. Saam, *Phys. Rev. Lett.* **75**, 4086 (1995).
- [27] E. Van Cleve, P. Taborek, and J. E. Rutledge, *J. Low Temp. Phys.* **150**, 1 (2008).
- [28] S. Curtarolo, M. W. Cole, and R. D. Diehl, *Phys. Rev. B* **70**, 115403 (2004).